

Dusty Debris Disks as Signposts of Planets: Implications for SIRTF

B. Zuckerman

ben@astro.ucla.edu

and

Inseok Song

song@astro.ucla.edu

Department of Physics and Astronomy

Center for Astrobiology

University of California, Los Angeles

Los Angeles, CA 90095–1562, USA

ABSTRACT

Submillimeter and near-infrared images of cool dusty debris disks and rings suggest the existence of unseen planets. At dusty but non-imaged stars, semi-major axes of associated planets can be estimated from the dust temperature. For some young stars these semi-major axes are greater than an arc second as seen from Earth. Such stars are excellent targets for sensitive near-infrared imaging searches for warm planets. To probe the full extent of the dust and hence of potential planetary orbits, SIRTF observations should include measurements with the $160\mu\text{m}$ filter.

Subject headings: (stars:) planetary systems — (stars:) planetary systems: protoplanetary disks — infrared: stars — astrobiology

1. Introduction

At near-infrared wavelengths, adaptive optics on 8 m class ground-based telescopes and the NICMOS camera on the Hubble Space Telescope can probe regions within a few arc seconds of nearby stars. In such regions, for stars younger than ~ 100 Myrs, warm massive planets can be detected. Dozens of such young stars within ~ 60 pc of Earth have been identified (Song *et al.* 2003; Zuckerman & Song 2004, and references therein).

Extant images at submillimeter and near-infrared wavelengths of cool dusty debris disks at main sequence stars (the so-called Vega phenomenon) usually show substantial spatial structure (e.g., Holland *et al.* 1998 & 2003; Greaves *et al.* 1998; Schneider *et al.* 1999; Krist *et al.* 2000; Koerner *et al.* 2001; Wilner *et al.* 2002; Weinberger *et al.* 2002 & 2003; Wahhaj *et al.* 2003; Clampin *et al.* 2003; Zuckerman 2001, and references therein). Specifically, the dusty

regions around ϵ Eri, Vega, Fomalhaut, β Pic, and HD 141569 all show obvious non-axisymmetric structure. HR 4796 is orbited by a narrow dusty ring. Only the dust at TW Hya has, so far, failed to reveal any structure of note.

Excepting perhaps HD 141569 (Clampin *et al.* 2003, and references therein), the most likely explanation of the observed structures are gravitational perturbations by planets with semi-major axes comparable to the radius of the dusty rings and disks. For Vega, a 3 Jupiter mass (M_J) planet is suggested (Wilner *et al.* 2002), while for ϵ Eri either a 0.2 M_J (Ozernoy *et al.* 2000) or a 0.1 M_J (Quillen & Thorndike 2002) planet has been proposed. Indeed, COBE found that Earth is led and trailed in its orbit around the Sun by clumps of dust particles (Reach *et al.* 1995). Additional discussions of planet/disk interactions can be found in Holland *et al.* (2003), Kenyon & Bromley (2002a, 2003), Kuchner & Holman (2003), Wyatt & Dent (2002), and Wyatt (2003).

Alternative mechanisms to generate structure in the dusty disks of other stars have been proposed, but likely account for very few, if any, of the observed structures. Kalas *et al.* (2001) investigated the possibility that a recent, close encounter with a passing star generated the structure observed in the northeast arm of the β Pic disk. While such an encounter might occur on rare occasions, such low-probability events cannot plausibly generate dusty structure in a high percentage of the Vega-like stars (e.g., Kenyon & Bromley 2002b). Takeuchi & Artymowicz (2001) proposed that ring structure, such as is observed at HR 4796 could be generated by dust particles migrating in an optically thin gaseous disk. This mechanism is implausible as an explanation for most, perhaps all, of the observed dusty structures because of (1) their often dramatic non-axisymmetric shape and (2) no evidence of gas at a majority of the above listed stars including even the model prototype HR 4796 (e.g., Zuckerman 2001, and references therein).

As a consequence of the above observations and arguments, one may reasonably assume that most stars with imaged dust emission have at least one planet on a wide orbit (tens of AU). From this assumption it follows that at stars with photometrically detected (but not yet imaged) dust there is a high probability of orbiting planets including at least one with a semi-major axis comparable to that of the dimensions of the dust disk.

Extrapolating from the preceding, one might speculate that young stars that do not have dust detectable by SIRTF do not possess planets on wide orbits (see discussion at end of Section 2). Although dust has not yet been measured directly in the Sun's Kuiper Belt, dust is very likely present and its presence is consistent with the existence of a planet (Neptune) at a roughly comparable distance from the Sun. Indeed, as has been pointed out by numerous researchers, with but few exceptions (e.g., Chen & Jura 2001), the dusty disks detected around main sequence stars (by IRAS and ISO) are likely analogs of the Kuiper Belt.

Twenty years ago, when IRAS first discovered the Vega-phenomenon, astronomers wondered whether a substantial link connected the presence of dust with planets. While stars with imaged dust remain frustratingly few in number, the common and striking structures that are seen now suggest that the link is substantial and that dusty stars represent excellent targets for planet searches.

For main sequence stars with circumstellar dust de-

tected by IRAS and/or ISO, the measured dust temperature is an indication of how far from a star the dust is located. In the following section we outline how the dust can be used to guide imaging planet searches and list specific stars at which to search.

2. Searching for planets at dusty stars

The IRAS database has been the prime source for identification of dusty main sequence stars. A few additional stars were added by ISO studies. A list of surveys for circumstellar dust appears in Section 3 of Zuckerman (2001) who remarked that, within certain constraints, the PhD thesis of Murray Silverstone (2000) represents the most comprehensive search to date of the IRAS catalogs for Vega-like stars.

In the discussion that follows and in Table 1, we focus primarily on stars listed in Silverstone's thesis. One of his constraints was that IRAS detected excess emission (due to the presence of dust) at $60\ \mu\text{m}$ wavelength. Thus, all stars in Table 1 are orbited by some dust that is sufficiently warm to radiate significantly at $60\ \mu\text{m}$. Table 1 also includes HIP 13402 and 71284 from Habing *et al.* (2001). Not all IR excess stars in Silverstone (2000) appear in our Table 1. For example, we excluded stars beyond 100 pc from Earth and stars with small dust optical depth τ (see below for definition of τ). We examined each putative excess star on the Digital Sky Survey plates and eliminated a few where it appears likely that the apparent far-IR stellar excess was instead emission from a galaxy near the star in the plane of the sky. We also have not included the big three (Vega, Fomalhaut, and β Pic) in Table 1. We felt that these have been analyzed and imaged to death already and we have nothing to add. The same might be said about ϵ Eri, but we included it in Table 1 because it well illustrates the conservative nature of the entries in columns 9 & 10 of Table 1 (see discussion below).

For Table 1 stars, we have constructed spectral energy distributions (SEDs) using optical, 2MASS, IRAS, and, when available, ISO fluxes. Synthetic stellar spectra of Hauschildt *et al.* (1999), $Z = 0.02$ and $\log g = 4.5$ model, are used in our SED fit process. Dust emission model parameters were found from eye-fitting model dust emission to IRAS (and ISO for some cases) measured fluxes (Figures 1–8). By assuming that the dust particles radiate like black bodies at temperature T_{dust} , one may derive their characteristic orbital radii (R_{dust}). These are indicated in column 9 of

Table 1, in Astronomical Units. Also indicated in Table 1 are the apparent angular radii (column 10) that characterize the dust distributions as seen from Earth.

R_{dust} was calculated from

$$R_{dust} = \left(\frac{R_{star}}{2} \right) \left(\frac{T_{star}}{T_{dust}} \right)^2$$

where R_{star} and T_{star} are given in columns 6 and 7 of Table 1 and are obtained from the SED fit and the distance D between Earth and star (column 5). We can check the accuracy of this technique directly for HIP 8102 (= τ Ceti) for which the VLT interferometer measured a stellar radius of $0.773 R_{\odot}$ (Pijpers *et al.* 2003); our technique yields $0.79 R_{\odot}$. An independent team of investigators (Kervella *et al.* 2003), who also use the VLT interferometer, report a radius of $0.804 R_{\odot}$ for HIP 8102. In addition, they measure $0.738 R_{\odot}$ for HIP 16537 (ϵ Eri); our technique yields $0.70 R_{\odot}$.

For many of the listed stars, these R_{dust} are “conservative” in that substantial amounts of dust might exist at larger distances. For example, particles at the IRAS color temperature that are small and radiate less effectively than black bodies in the far-IR will be located further from the star than indicated in Table 1. Also, particles that are too cold to radiate much at $60 \mu\text{m}$ would not have been detected by IRAS.

Zuckerman & Becklin (1993) deduced that, for the A-type stars Vega, Fomalhaut and β Pic, there is not much dust too cold to have been detected by IRAS. This conclusion was confirmed by Holland *et al.* (1998) and by Harvey & Jefferys (2000). In addition, Holland *et al.* noted that the dominant radiating particles at Fomalhaut appear to be behaving like black bodies.

In contrast, at some stars there is substantial evidence (summarized in Section 4.2 of Zuckerman 2001) for particles at larger distances than implied by the IRAS color temperature and the blackbody assumption. The characteristic dust orbital radius (19 AU) calculated (Table 1) from the IRAS color temperature for the K2 star ϵ Eri (HIP 16537) is a few times smaller than the radius of the dust ring imaged by Greaves *et al.* (1998) at $800 \mu\text{m}$ wavelength. Should dust be present $\gtrsim 100$ AU from late-type stars, then such stars are insufficiently luminous to heat all surrounding dust to the ~ 30 K required for generation of substantial $60 \mu\text{m}$ emission. For example, a G0 star can heat large (black-body) particles to ~ 30 K at a distance of

100 AU. The corresponding distances for K0 and M0 stars are only ~ 65 and 25 AU, respectively.

In addition, even for some early-type stars, our expression for R_{dust} will underestimate the true extent of the dust distribution. For example, at HR 4796, our SED fit implies R_{star} , T_{star} , and T_{dust} of $1.86 R_{\odot}$, 9200 K, and 100 K respectively, which yields a calculated $R_{dust} = 37$ AU. However, the radius of the dusty ring imaged by NICMOS with the Space Telescope is ~ 65 AU (see, e.g., Figure 1 in Zuckerman 2001).

In column 11 of Table 1, τ is the total energy emitted by dust grains divided by the bolometric luminosity of the star. τ is a measure of the fraction of the ultraviolet and visual light emitted by the star that is absorbed by the orbiting dust particles. The listed values of τ , which are obtained from the SEDs shown in Figures 1–8, usually agree reasonably well with values of τ given in Silverstone (2000), although discrepancies of a factor of two or three sometimes appear. τ may be used as one age indicator. From Spangler *et al.* (2001), if $\tau \gtrsim 0.001$, then a star is probably not older than ~ 100 Myrs. It may be seen that most stars in Table 1 with multiple age indicators conform to this rule, but there are a few potential exceptions, notably HIP 35457, 69682, & 87815.

Additional techniques for estimating stellar ages are listed in Zuckerman *et al.* (2001a) and Song *et al.* (2003). We used a variety of techniques, indicated in column 13 of Table 1, to deduce the ages in column 12. Some of the ages are quite secure, others not so secure (one question mark), or quite uncertain (two question marks).

Planet detection with current adaptive optics (AO) imaging systems on large telescopes requires planet-star separations of at least one to two arc seconds. In addition, a planet must be sufficiently warm to radiate at near-IR wavelengths. Long integrations on nearby stars with ages of hundreds of millions of years can probe down to a few Jupiter masses (e.g., Macintosh *et al.* 2003). Ages of tens of millions of years or less are required if planets of a Jupiter mass are to be detected. Thus, to optimize imaging planet searches accurate stellar ages are required.

Because AO (and HST/NICMOS) sensitivities are telescope, elevation, and wavelength specific and because H , K' , and L' thermal fluxes from planets with temperatures $\lesssim 700$ K are based on model predictions and not on observations, it is not possible to give a general prescription regarding which stars in Table 1

should be observed with AO and at what wavelength. Indeed an AO system has been commissioned on the VLT only within the past year and Gemini North and South and Subaru have had no or only rudimentary AO systems.

That said, for a given star/dust angular separation (column 10 in Table 1), planet detectability is maximized by observing the youngest, closest stars to Earth. For example, a two Jupiter mass planet will fade by 5-6 magnitudes, in an absolute sense and also relative to the brightness of its star, at H and K bands as it ages from 10 to 100 Myrs. Similarly, a planet 50 pc from Earth will be 3.5 magnitudes fainter than a comparably warm one only 10 pc away (while the star/planet contrast is independent of distance). Then there is stellar spectral type to consider. A planet of given mass, age, and semi-major axis will be harder to detect close to an intrinsically luminous A-type star compared to one of K-type. But if more massive planets, perhaps with larger semi-major axes, form near the relatively more massive stars, then this might more than compensate for the unfavorable contrast ratio. In any event, because AO systems (unlike HST/NICMOS) are not well suited to detection of extended objects, near infrared light scattered by dust, even for stars with large τ , is very unlikely to hamper planet detection.

Both observation (Spangler *et al.* 2001) and theory suggest that, on average, young stars will have a dustier “Kuiper Belt” than old stars. Based on the mass of Neptune, the mass ($\sim 3M_{Neptune}$) of the proposed planet on a wide orbit at ϵ Eri, and the decrease of τ with time indicated in Figure 2 of Spangler *et al.* (2001), a star of age \lesssim few 100 million years with a similarly massive planet on a wide orbit would have $\tau \gtrsim 10^{-5}$. SIRTF should generally be capable of detecting τ as small as 10^{-6} . Thus, if the dust-planet connection is as strong as we suggest, then Jupiter mass planets on wide orbits will rarely, if ever, be detected around young stars that lack SIRTF detected far-IR excess emission. The same may be true for Saturn or even Neptune mass planets, although these, of course, will be much harder to detect.

3. Conclusions

Recent imaging observations and analysis of structure in the dusty debris disks that surround a handful of nearby stars suggest that they possess planets on wide orbits (tens of AU). Thus, dusty stars, whether imaged

or not, are excellent targets for planet searches. Young stars with cool dust make the best targets for adaptive optics and HST imaging programs. Older stars and those with somewhat warmer dust might be better investigated with precision radial velocities. While the earliest searches of the IRAS catalogs revealed mostly A-type Vega-like stars which are not suitable for study by the precision radial velocity technique, a majority of stars in Table 1 are of later spectral types.

Looking toward the future, one anticipates that SIRTF will search for dusty debris at all nearby stars that have been identified as very young (e.g., Zuckerman et al 2001a, Song et al 2003). Since the presence of cool dust would point toward the existence of planets on wide orbits accessible to adaptive optics, it is important that the SIRTF programs include measurements with the 160 μm filter.

We thank Dr. Murray Silverstone for information regarding the relative positions of IRAS 12 & 60 μm sources, and Drs. M. Jura, E. Becklin, and B. Macintosh for helpful comments. This research was supported by a NASA grant to UCLA and by NASA’s Astrobiology Institute.

REFERENCES

- Chen, C. H. & Jura, M. 2001, *ApJ*, **560**, L171
- Clampin, M., *et al.* 2003, *AJ*, **126**, 385
- Greaves, J. S., *et al.* 1998, *ApJ*, **506**, L133
- Habing, H. J., *et al.* 2001, *A&A*, **365**, 545
- Harvey, P. M. & Jefferys, W. H. 2000, *ApJ*, **538**, 783
- Hauschildt, P. H., Allard, F., Ferguson, J., Baron, E., & Alexander, D. R. 1999, *ApJ*, **525**, 871
- Holland, W. S., *et al.* 1998, *Nature*, **392**, 788
- 2003, *ApJ*, **582**, 1141
- Kalas, P., Deltorn, J., & Larwood, J. 2001, *ApJ*, **553**, 410
- Kenyon, S. J. & Bromley, B. C. 2002a, *ApJ*, **577**, L35
- Kenyon, S. J. & Bromley, B. C. 2002b, *AJ*, **123**, 1757
- Kenyon, S. J. & Bromley, B. C. 2003, ArXiv Astrophysics e-prints, 9540

Kervella, P. et al. 2003, ArXiv Astrophysics e-prints, 9784

Koerner, D. W., Sargent, A. I., & Ostroff, N. A. 2001, *ApJ*, **560**, L181

Krist, J. E., Stapelfeldt, K. R., Ménard, F., Padgett, D. L., & Burrows, C. J. 2000, *ApJ*, **538**, 793

Kuchner, M. J. & Holman, M. J. 2003, *ApJ*, 588, 1110

Lowrance, P. J., et al. 2000, *ApJ*, **541**, 390

Macintosh, B., Becklin, E. E., Kaisler, D., Konopacky, Q., & Zuckerman, B. 2003, *ApJ*, 594, 538

Ozernoy, L. M., Gorkavyi, N. N., Mather, J. C., & Taidakova, T. A. 2000, *ApJ*, **537**, L147

Pijpers, F. P., Teixeira, T. C., Garcia, P. J., Cunha, M. S., Monteiro, M. J. P. F. G., & Christensen-Dalsgaard, J. 2003, *A&A*, **406**, L15

Quillen, A. C. & Thorndike, S. 2002, *ApJ*, **578**, L149

Reach, W. T., et al. 1995, *Nature*, **374**, 521

Schneider, G., et al. 1999, *ApJ*, **513**, L127

Silverstone, M. 2000, *PhD Thesis*, UCLA

Song, I., Bessell, M. S., & Zuckerman, B. 2002, *A&A*, **385**, 862 (SBZ)

Song, I., Caillault, J.-P., Barrado y Navascués, D., & Stauffer, J. R. 2001, *ApJ*, **546**, 352 (S2001)

Song, I., Caillault, J.-P., Barrado y Navascués, D., Stauffer, J. R., & Randich, S. 2000, *ApJ*, **533**, L41 (S2000)

Song, I., Zuckerman, B., & Bessell, M. S. 2003, *ApJ*, in press, Dec 10 (SZB)

Spangler, C., Sargent, A. I., Silverstone, M. D., Becklin, E. E., & Zuckerman, B. 2001, *ApJ*, **555**, 932

Takeuchi, T. & Artymowicz, P. 2001, *ApJ*, **557**, 990

Wahhaj, Z., Koerner, D. W., Ressler, M. E., Werner, M. W., Backman, D. E., & Sargent, A. I. 2003, *ApJ*, **584**, L27

Weinberger, A. J., Becklin, E. E., & Zuckerman, B. 2003, *ApJ*, **584**, L33

Weinberger, A. J., et al. 2002, *ApJ*, **566**, 409

Wilner, D. J., Holman, M. J., Kuchner, M. J., & Ho, P. T. P. 2002, *ApJ*, **569**, L115

Wyatt, M. C. 2003, ArXiv Astrophysics e-prints, 8253

Wyatt, M. C. & Dent, W. R. F. 2002, *MNRAS*, 334, 589

Zuckerman, B. 2001, *ARA&A*, **39**, 549

Zuckerman, B. & Becklin, E. E. 1993, *ApJ*, **414**, 793

Zuckerman, B., Forveille, T., & Kastner, J. H. 1995, *Nature*, **373**, 494 (ZFK)

Zuckerman, B. & Song, I. 2004, *ARA&A*, **42**, in press

Zuckerman, B., Song, I., Bessell, M. S., & Webb, R. A. 2001a, *ApJ*, **562**, L87 (ZSBW)

Zuckerman, B., Song, I., & Webb, R. A. 2001b, *ApJ*, **559**, 388 (ZSW)

Zuckerman, B. & Webb, R. A. 2000, *ApJ*, **535**, 959 (ZW)

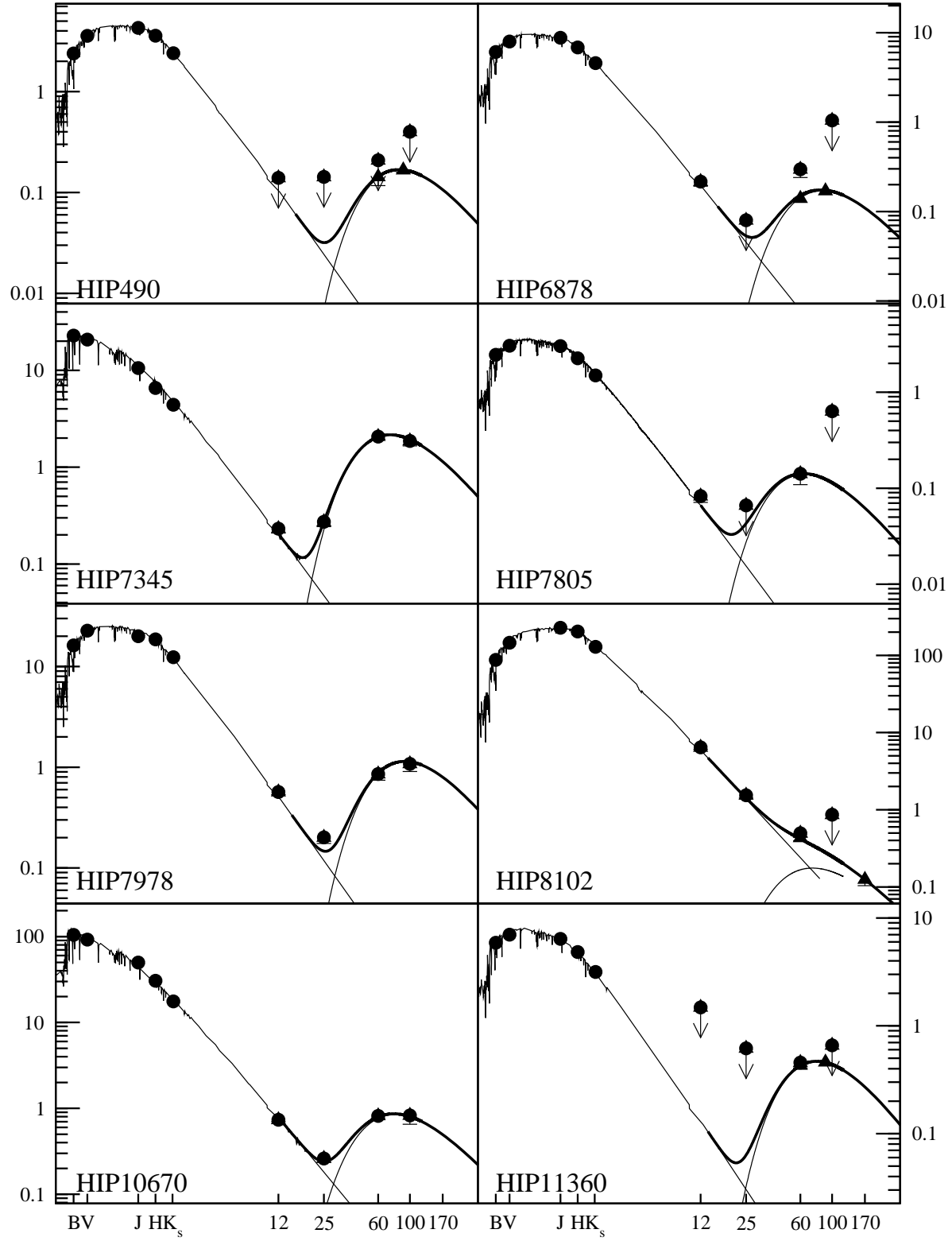


Fig. 1.— Spectral energy distributions of stars with dusty debris disks. B & V fluxes from Hipparcos, JHK_s from 2MASS, 12/25/60/100 μm from IRAS. In addition, 60/90/100/170 μm fluxes (triangles) from ISO.

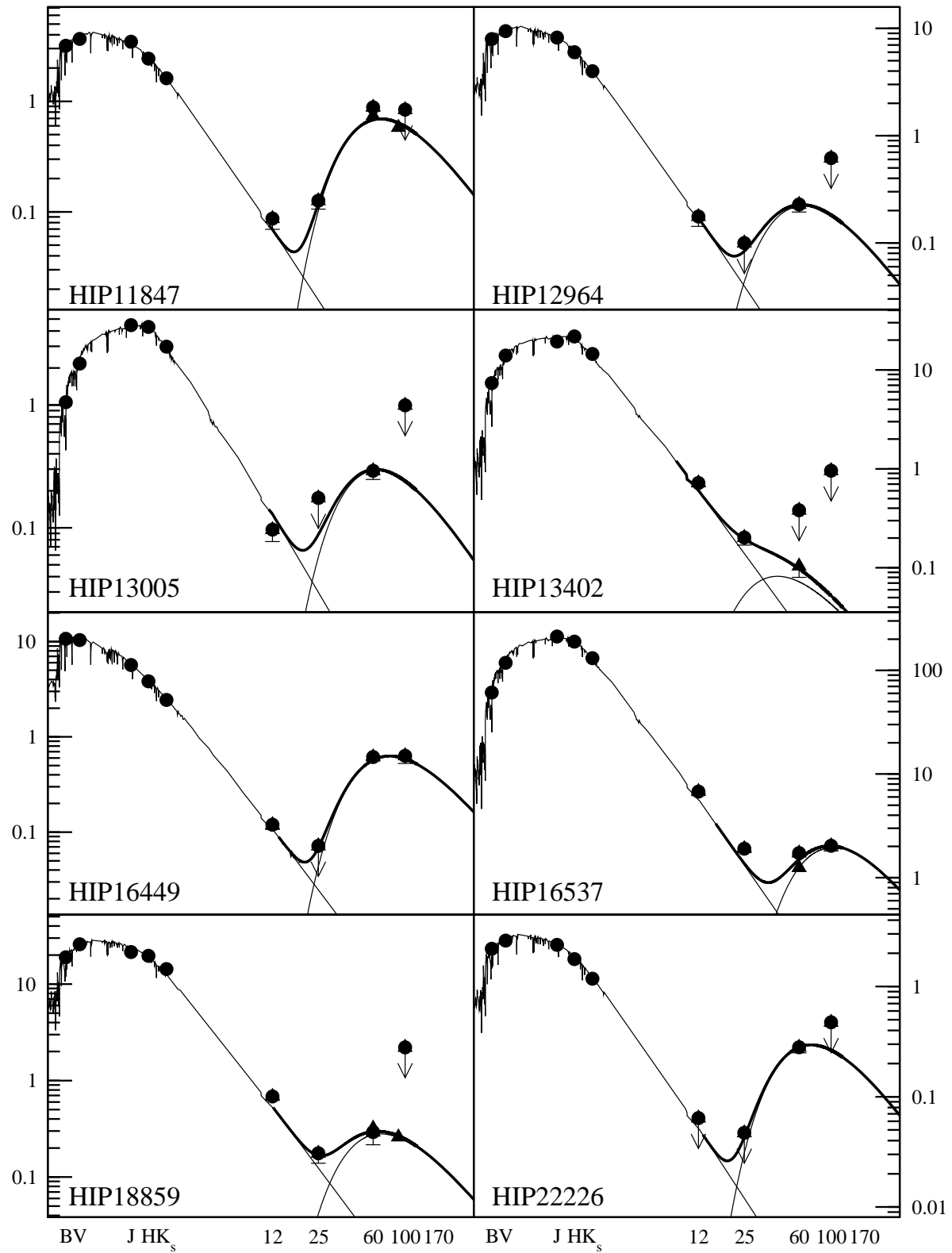


Fig. 2.— Spectral energy distributions of stars with dusty debris disks (See caption to Figure 1)

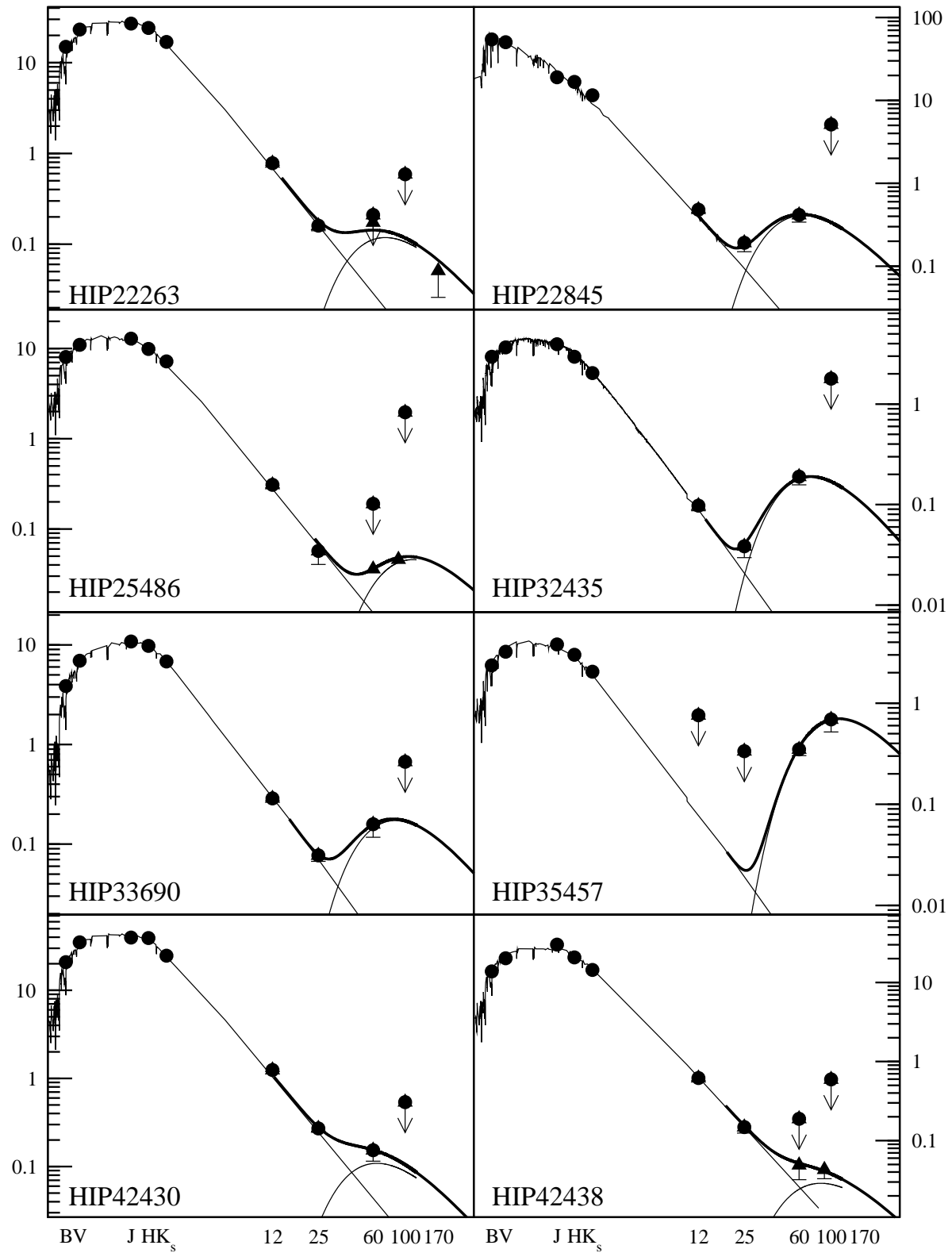


Fig. 3.— Spectral energy distributions of stars with dusty debris disks (See caption to Figure 1).

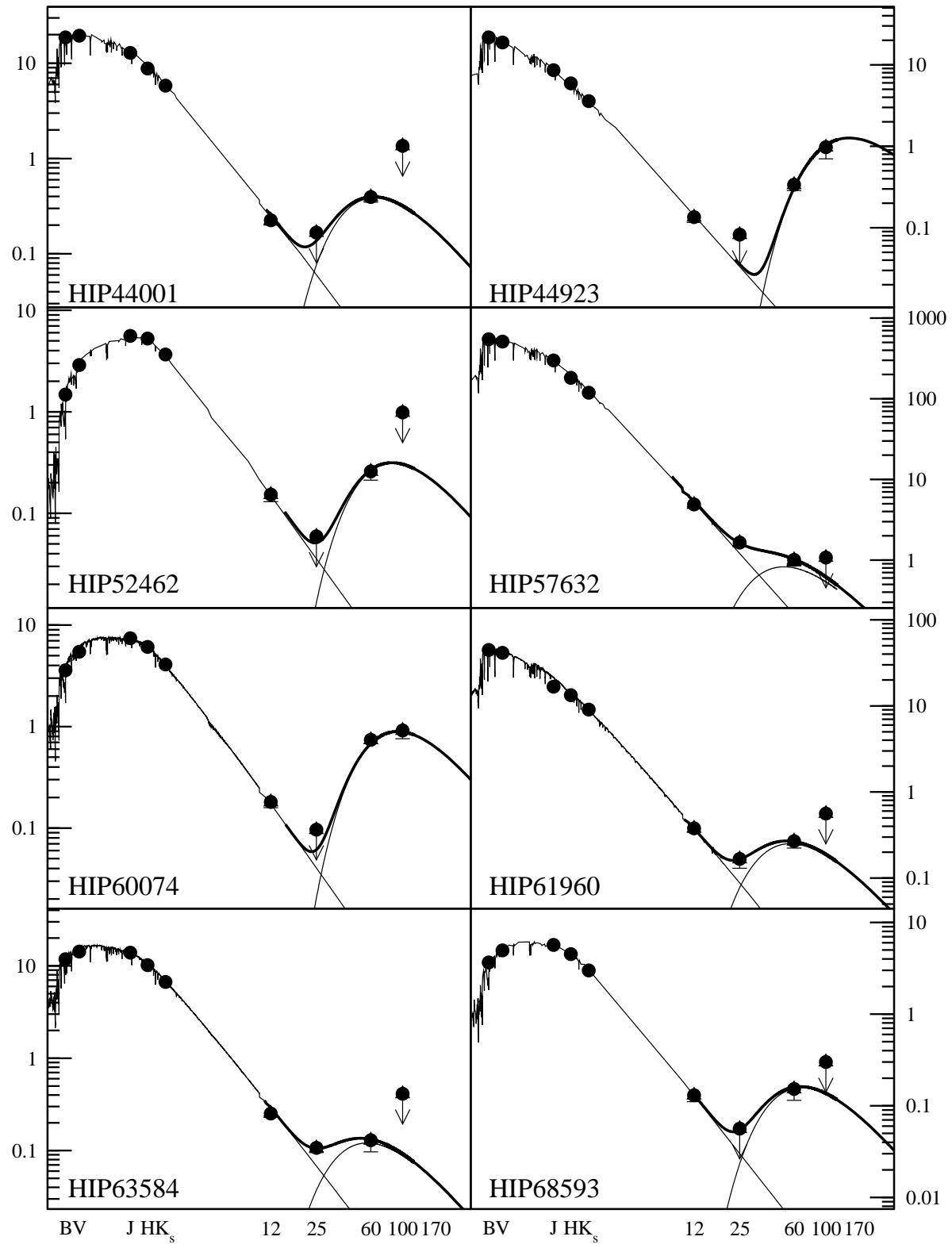


Fig. 4.— Spectral energy distributions of stars with dusty debris disks (See caption to Figure 1).

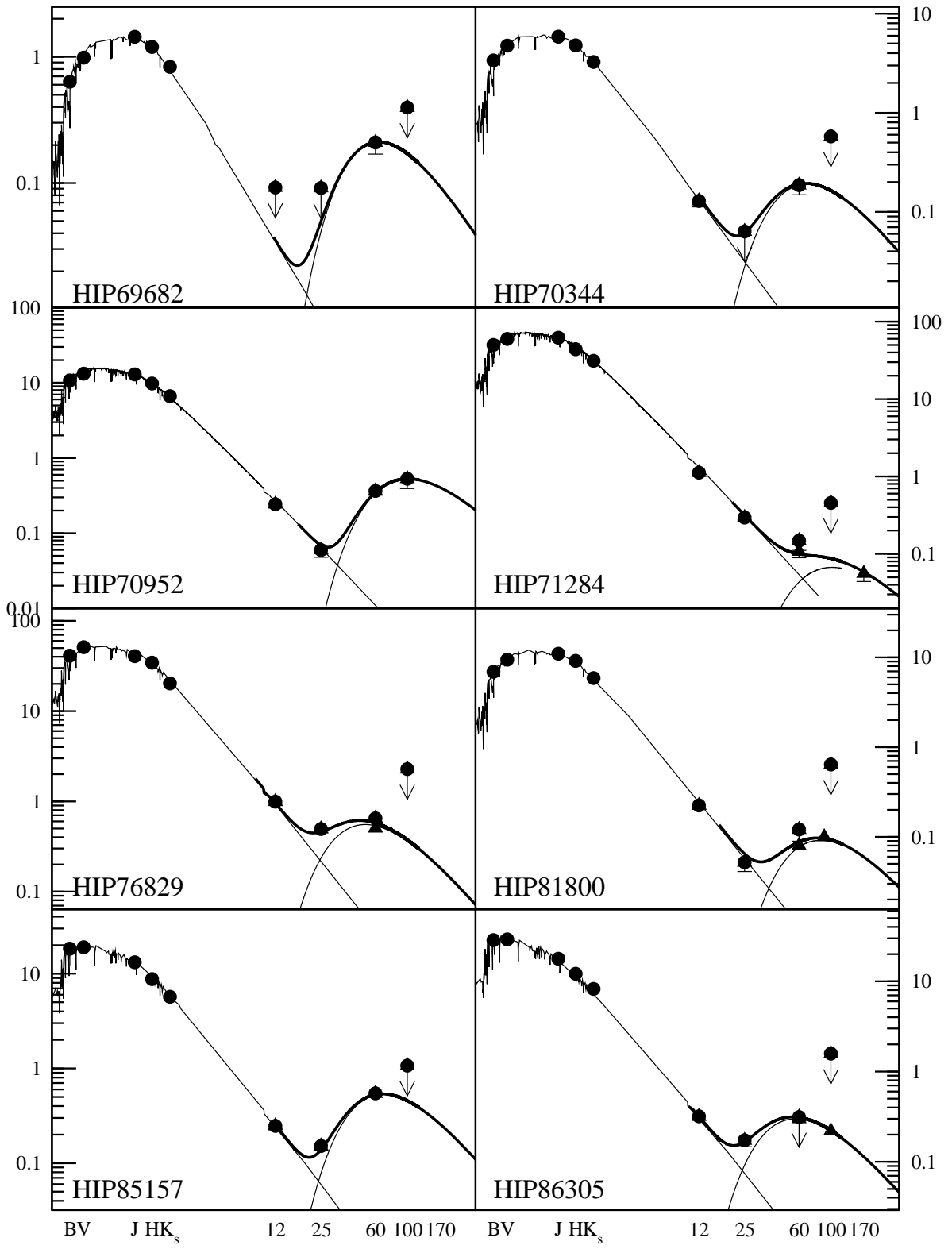


Fig. 5.— Spectral energy distributions of stars with dusty debris disks (See caption to Figure 1). 60 and 100 μm fluxes (triangles) for HIP 86305 from Silverstone (2000).

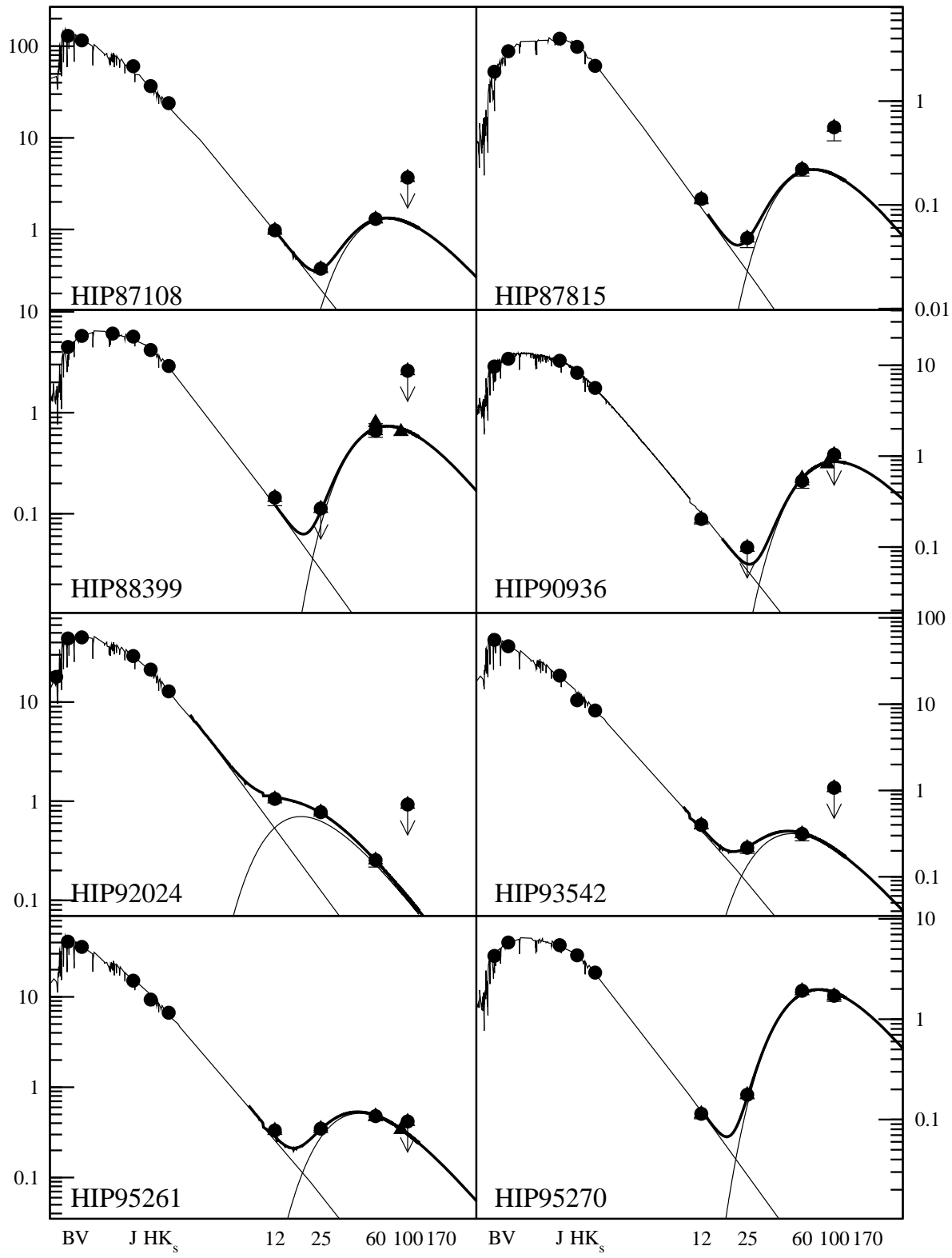


Fig. 6.— Spectral energy distributions of stars with dusty debris disks (See caption to Figure 1).

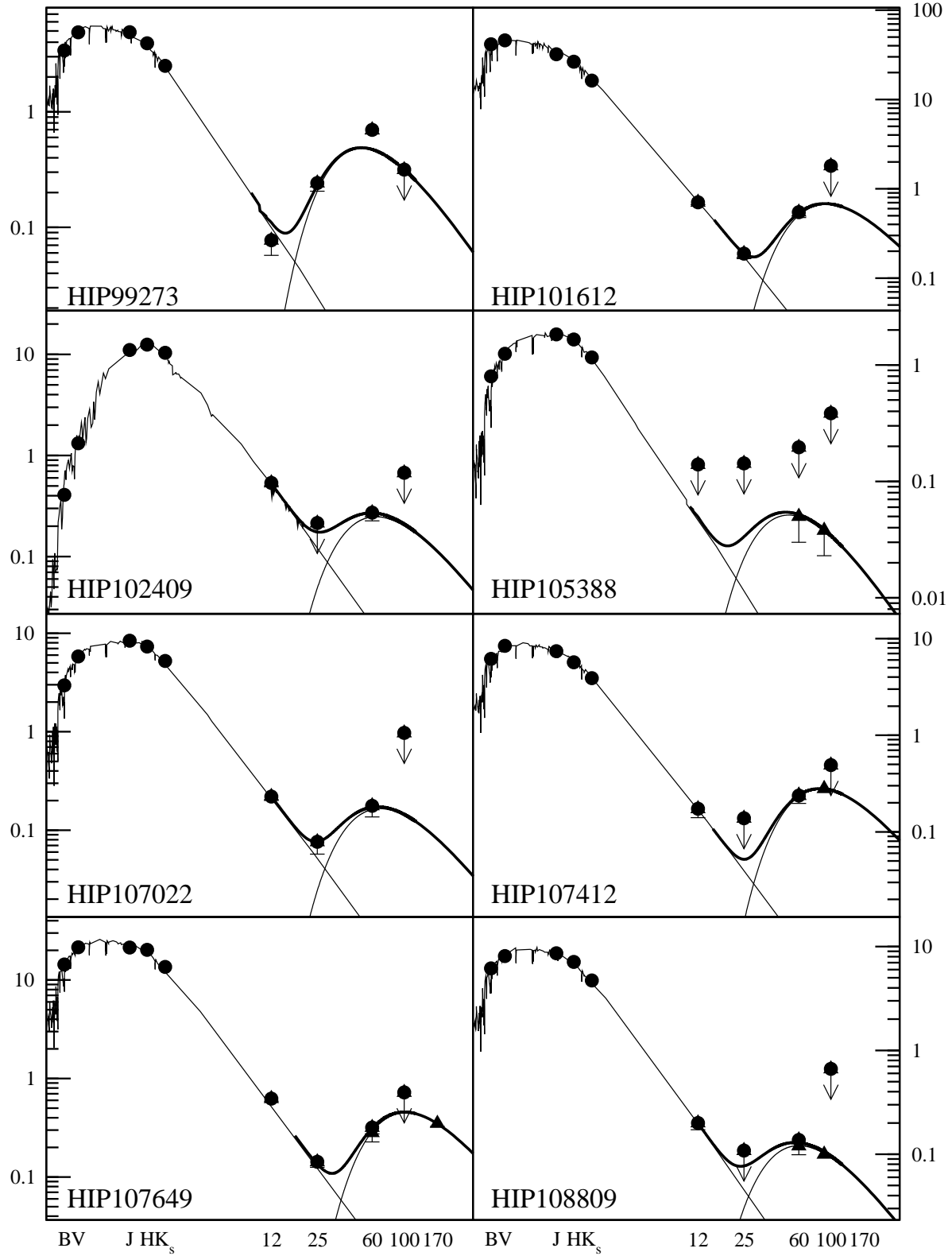


Fig. 7.— Spectral energy distributions of stars with dusty debris disks (See caption to Figure 1).

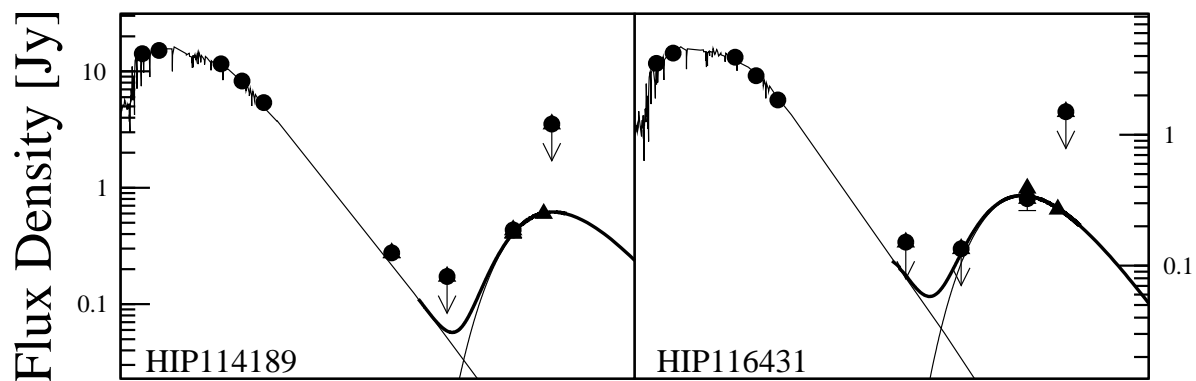


Fig. 8.— Spectral energy distributions of stars with dusty debris disks (See caption to Figure 1).

Table 1:: Stars with Dusty Debris Disks

| HIP | HD | Sp. Type | V [mag] | D [pc] | R_{star} $[R_{\odot}]$ | T_{star} [K] | T_{dust} [K] | R_{dust} [AU] | angle [""] | $\tau \times 10^{-4}$ | age [Myrs] | age method | notes |
|-------|--------|-------------|------------|-----------|-----------------------------|-------------------|-------------------|--------------------|---------------|-----------------------|----------------|------------|-------|
| (1) | (2) | (3) | (4) | (5) | (6) | (7) | (8) | (9) | (10) | (11) | (12) | (13) | (14) |
| 490 | 105 | G0V | 7.5 | 40.2 | 1.16 | 5800 | 60 | 27 | 0.68 | 5 | $\lesssim 100$ | a,b,c | 1 |
| 6878 | 8907 | F8 | 6.7 | 34.2 | 1.34 | 5800 | 60 | 31 | 0.92 | 3 | 200? | a,b,c | 1 |
| 7345 | 9672 | A1V | 5.6 | 61.3 | 1.96 | 8600 | 70 | 74 | 1.21 | 6 | 20? | ZFK | 2 |
| 7805 | 10472 | F2IV/V | 7.7 | 66.6 | 1.40 | 6400 | 80 | 22 | 0.34 | 6 | 30 | ZSW | |
| 7978 | 10647 | F8V | 5.5 | 17.4 | 0.99 | 6200 | 55 | 31 | 1.81 | 3 | 300? | a,b,c | |
| 8102 | 10700 | G8V | 3.6 | 3.6 | 0.79 | 5400 | 70 | 12 | 3.26 | 0.1 | 7000?? | a,b | 1 |
| 10670 | 14055 | A1Vnn | 4.0 | 36.1 | 2.09 | 9400 | 65 | 109 | 3.03 | 0.6 | 100? | a,d | |
| 11360 | 15115 | F2 | 6.8 | 44.8 | 1.30 | 6800 | 65 | 36 | 0.79 | 5 | 100? | a,b,c | 1 |
| 11847 | 15745 | F0 | 7.5 | 63.7 | 1.30 | 6800 | 75 | 27 | 0.42 | 12 | 30? | d,e | 1 |
| 12964 | 17390 | F3IV/V | 6.6 | 45.1 | 1.47 | 6800 | 80 | 27 | 0.59 | 2 | 300?? | a | |
| 13005 | — | K0 | 8.1 | 67.7 | 2.22 | 5000 | 60 | 39 | 0.57 | 14 | ? | b,e | 3 |
| 13402 | 17925 | K1V | 6.0 | 10.4 | 0.73 | 5200 | 60 | 14 | 1.32 | 0.8 | $\lesssim 100$ | a,b,c | 1 |
| 16449 | 21997 | A3IV/V | 6.7 | 73.8 | 1.64 | 8400 | 65 | 68 | 0.93 | 3 | 100? | d | |
| 16537 | 22049 | K2V | 3.7 | 3.2 | 0.70 | 5200 | 50 | 19 | 5.90 | 0.7 | 730 | S2000 | 1 |
| 18859 | 25457 | F5V | 5.4 | 19.2 | 1.15 | 6400 | 75 | 21 | 1.09 | 0.8 | 30 | a,b,c | 1 |
| 22226 | 30447 | F3V | 7.9 | 78.1 | 1.31 | 6600 | 70 | 29 | 0.37 | 11 | $\lesssim 100$ | e | |
| 22263 | 30495 | G3V | 5.5 | 13.3 | 0.99 | 5600 | 70 | 16 | 1.19 | 0.6 | 300? | a,b | 1 |
| 22845 | 31295 | A0V | 4.6 | 37.0 | 1.56 | 9400 | 80 | 54 | 1.45 | 0.3 | 100? | a,d | |
| 25486 | 35850 | F7V: | 6.3 | 26.8 | 1.24 | 6000 | 45 | 55 | 2.06 | 0.2 | 12 | ZSBW | 1 |
| 32435 | 53842 | F5V | 7.5 | 57.3 | 1.46 | 6200 | 70 | 29 | 0.50 | 4.5 | 30? | a,b,c | |
| 33690 | 53143 | K0IV/V | 6.8 | 18.4 | 0.92 | 5200 | 60 | 17 | 0.94 | 2.5 | 300? | a,b,c | |
| 35457 | 56099 | F8 | 7.6 | 86.8 | 2.17 | 6200 | 45 | 70 | 0.80 | 12 | $> 500?$ | a,b,e | 4 |
| 42430 | 73752 | G3/5V | 5.0 | 19.9 | 1.83 | 5600 | 80 | 17 | 0.83 | 0.3 | > 600 | S2000 | 5 |
| 42438 | 72905 | G1.5Vb | 5.6 | 14.3 | 0.99 | 5800 | 60 | 23 | 1.62 | 0.1 | 200? | a,b,c | 1 |
| 44001 | 76582 | F0IV | 5.7 | 49.3 | 1.89 | 7600 | 80 | 43 | 0.85 | 3 | 300?? | a,d | |
| 44923 | 78702 | A0/1V | 5.9 | 79.9 | 2.13 | 9600 | 35 | 400 | 5.00 | 2.5 | 100? | d | |
| 52462 | 92945 | K1V | 8.0 | 21.6 | 0.81 | 5000 | 60 | 14 | 0.65 | 7 | 100 | SBZ | |
| 57632 | 102647 | A3Vvar | 2.1 | 11.1 | 1.81 | 8400 | 100 | 32 | 2.90 | 0.2 | 50 | S2001 | |
| 60074 | 107146 | G2V | 7.0 | 28.5 | 1.02 | 5800 | 55 | 28 | 1.00 | 12 | $\lesssim 100$ | a,b,c,e | |
| 61960 | 110411 | A0V | 4.9 | 36.9 | 1.55 | 8800 | 90 | 37 | 1.00 | 0.3 | 100?? | a,d | |
| 63584 | 113337 | F6V | 6.0 | 37.4 | 1.67 | 6600 | 90 | 22 | 0.60 | 1 | 50? | a,b | 6 |
| 68593 | 122652 | F8 | 7.2 | 37.2 | 1.18 | 6000 | 75 | 19 | 0.51 | 3 | 300? | a,b,c | |
| 69682 | 124718 | G5V | 8.9 | 61.3 | 1.03 | 5600 | 80 | 13 | 0.21 | 27 | > 500 | a,b,c,e | 7 |

continued on next page

Table 1:: (continued)

| HIP | HD | Sp. | V | D | R_{star} | T_{star} | T_{dust} | R_{dust} | angle | τ | age | age method | notes |
|--------|--------|--------|-----|------|------------|------------|------------|------------|-------|--------|----------------|------------|-------|
| 70344 | 126265 | G2III | 7.2 | 70.1 | 2.31 | 5800 | 75 | 35 | 0.50 | 2 | > 500 | a,b | |
| 70952 | 127821 | F4IV | 6.1 | 31.7 | 1.35 | 6600 | 50 | 59 | 1.84 | 1.5 | 200? | a,b | |
| 71284 | 128167 | F3Vvar | 4.5 | 15.5 | 1.46 | 6400 | 50 | 60 | 3.86 | 0.1 | 1000?? | a,b,c | 1 |
| 76829 | 139664 | F5IV/V | 4.6 | 17.5 | 1.38 | 6600 | 100 | 15 | 0.86 | 0.9 | 200? | a,b,c | 1 |
| 81800 | 151044 | F8V | 6.5 | 29.4 | 1.26 | 6000 | 60 | 32 | 1.09 | 0.8 | > 500 | a,b | 1 |
| 85157 | 157728 | F0IV | 5.7 | 42.8 | 1.63 | 7600 | 75 | 42 | 0.97 | 3 | 100? | a,d | |
| 86305 | 159492 | A7V | 5.2 | 42.2 | 1.75 | 8200 | 90 | 36 | 0.87 | 1 | 200? | a,d | 1 |
| 87108 | 161868 | A0V | 3.8 | 29.1 | 1.92 | 9400 | 70 | 87 | 2.97 | 0.6 | 200? | a,d | |
| 87815 | 164330 | K0 | 7.7 | 83.2 | 2.30 | 5600 | 70 | 37 | 0.44 | 9 | > 500 | a,b,e | |
| 88399 | 164249 | F5V | 7.0 | 46.9 | 1.36 | 6400 | 70 | 28 | 0.60 | 19 | 12 | ZSBW | 1 |
| 90936 | 170773 | F5V | 6.3 | 36.1 | 1.45 | 6600 | 50 | 63 | 1.75 | 5 | 200? | a,b,c | 1 |
| 92024 | 172555 | A7 | 4.8 | 29.2 | 1.61 | 7800 | 280 | 3 | 0.11 | 5 | 12 | ZSBW | |
| 93542 | 176638 | A0Vn | 5.1 | 56.3 | 2.33 | 9800 | 100 | 56 | 1.00 | 0.7 | 200? | a,d | |
| 95261 | 181296 | A0Vn | 5.0 | 47.7 | 1.63 | 9800 | 110 | 32 | 0.68 | 0.8 | 12 | ZSBW | 1 |
| 95270 | 181327 | F5.5V | 7.0 | 50.6 | 1.44 | 6400 | 65 | 35 | 0.68 | 32 | 12 | ZSBW | |
| 99273 | 191089 | F5V | 7.5 | 53.5 | 1.40 | 6400 | 100 | 14 | 0.27 | 13 | $\lesssim 100$ | a,b,c,e | |
| 101612 | 195627 | F1III | 4.5 | 27.6 | 1.86 | 7000 | 55 | 75 | 2.69 | 1 | 200? | a,d | |
| 102409 | 197481 | M1Ve | 8.8 | 9.9 | 0.76 | 3800 | 80 | 4 | 0.43 | 1 | 12 | ZSBW | |
| 105388 | 202917 | G5V | 8.7 | 45.9 | 0.94 | 5400 | 100 | 7 | 0.15 | 6 | 30 | ZW | 1 |
| 107022 | 205536 | G8V | 7.1 | 22.1 | 0.93 | 5800 | 75 | 14 | 0.63 | 3 | > 500 | a,b | |
| 107412 | 206893 | F5V | 6.9 | 38.9 | 1.30 | 6400 | 60 | 37 | 0.95 | 2 | 200? | a,b | 1 |
| 107649 | 207129 | G2V | 5.6 | 15.6 | 0.98 | 6000 | 50 | 35 | 2.26 | 1.4 | 600 | SZB | 1 |
| 108809 | 209253 | F6/7V | 6.9 | 30.1 | 1.09 | 6200 | 85 | 14 | 0.48 | 0.9 | 200?? | a,b,c | 1 |
| 114189 | 218396 | A5V | 6.0 | 39.9 | 1.42 | 7400 | 50 | 78 | 1.95 | 1.4 | 30 | a,d | 1 |
| 116431 | 221853 | F0 | 7.3 | 71.2 | 1.66 | 6600 | 90 | 22 | 0.31 | 12 | $\lesssim 100$ | e | 1 |

Footnotes to Table 1.

– Age Methods::

- S2000=Song *et al.* (2000)
- S2001=Song *et al.* (2001)
- SBZ= Song *et al.* (2002)
- ZFK =Zuckerman *et al.* (1995)
- ZSBW=Zuckerman *et al.* (2001a)
- ZSW =Zuckerman *et al.* (2001b)
- ZW= Zuckerman & Webb (2000)
- SZB =Song *et al.* (2003)
- a UVW (Zuckerman & Song 2004)
- b X-ray emission (e.g., Song *et al.* 2003)
- c lithium age (Song *et al.* 2003)
- d location on an A-star Hertzsprung-Russell diagram (Lowrance *et al.* 2000)
- e dust (if $\tau \gtrsim 10^{-3}$, then age $\lesssim 10^8$ years, Spangler *et al.* 2001)

– Calculations use 1 AU=200 R_{\odot}

Notes to Table 1.

1. ISO 60, 90, 100, and/or $170\mu\text{m}$ fluxes available from Silverstone (2000) and/or Habing *et al.* (2001); see Figures 1–8.
2. HIP 7345 (=49 Cet) is the only known main sequence A-type star with CO emission detected with a radio telescope (ZFK), thus suggesting a very young age. But its galactic space motion UVW ($-23, -17, -4$) with respect to Sun is not indicative of extreme youth (U is positive toward the Galactic center).
3. Based on the offset between the 12 and $60\mu\text{m}$ IRAS positions, the apparent $60\mu\text{m}$ excess is probably from a galaxy at position angle $\sim 70^\circ$ and $\sim 45''$ from HIP 13005.
4. HIP 35457 is a $0.^{\prime\prime}16$ binary. The very large τ seems inconsistent with the old age implied by the absence of ROSAT All Sky X-ray emission and the stars' galactic space motion (UVW).
5. HIP 42430 is a $1.^{\prime\prime}0$ binary.
6. M-star companion LDS 2662 is very young based on its location on an M_K versus $V-K$ color magnitude diagram (e.g., Figure 2 in SZB).
7. The Galactic space motion (UVW) and absence of lithium and of X-ray emission all point to an old star. There is no evidence on the Digital Sky Survey and 2MASS All Sky QuickLook Images (JHK_s) of a nearby galaxy. Yet τ is very large.